J. Synchrotron Rad. (1998). **5**, 1187–1194

Relationship Between Spatial Coherence of Synchrotron Radiation and Emittance

Y. Takayama,[a]* T. Hatano,[b] T. Miyahara[c] and W. Okamoto[d]

[a]Department of Synchrotron Radiation Science, Graduate University of Advanced Studies, 1-1 Oho, Tsukuba, Ibaraki 305, Japan, [b]Research Institute for Scientific Measurement, Tohoku University, 2-1-1 Katahira Aobaku, Sendai 980-77, Japan, [c]Department of Physics, Faculty of Science, Tokyo Metropolitan University, 1-1 Minami-Ohsawa, Hachioji, Tokyo 192-03, Japan, and [d]Photon Factory, Institute of Materials Structure Science, 1-1 Oho, Tsukuba, Ibaraki 305, Japan. E-mail: taka@powerpc4.kek.jp

(*Received 24 September 1997; accepted 17 December 1997*)

Analytical calculation of the first-order spatial coherence for the Gaussian beam and the exact numerical calculation for synchrotron radiation are compared in this paper. The approximation of regarding synchrotron radiation as a Gaussian beam is often used to investigate the brightness, the flux and some qualitative properties. Calculations show that synchrotron radiation does not have as high coherence as the Gaussian beam because of the beam profile, the phases of the wave and the polarization. If one can measure the beam size and the spatial coherence of synchrotron radiation, it is possible to determine the total photon beam emittance without any knowledge of the Twiss parameters of the ring.

Keywords: coherence; visibility; emittance; Gaussian beam.

1. Introduction

Coherence is one of the most important properties of wave optics. There are two concepts for coherence. One is the spatial coherence which represents how the fields at two points in a plane perpendicular to the optical axis can interfere. The other is the temporal coherence which is equivalent to the length of the wave packet. We have constructed a Young's interferometer to measure the first-order coherence of synchrotron radiation in the soft X-ray region (Hatano *et al.*, 1998). Some measurements have been performed at BL-12A (a bending-magnet beamline) and BL-28A (a helical-undulator beamline) of the Photon Factory, KEK. We can see the great difference between the visibilities in the vertical and horizontal directions which is due to the difference between the electron beam emittances in the storage ring. From the van Cittert–Zernike theorem (Mandel & Wolf, 1995) one can gain knowledge of the intensity distribution of the light source by measuring the spatial coherence of the far field for ordinary light sources. In this theorem, light from each point source is often treated as a spherical wave and has a finite size but no directional dependence, which is not true for synchrotron radiation. However, by approximating the synchrotron radiation as a Gaussian beam one can obtain an analytical representation of the visibility. For simple cases, some calculations of the spatial coherence are performed in the far-field approximation (Coisson, 1995). In this paper we will present the analytical calculation of the coherence for the Gaussian beam in the linear approximation and compare the result with the numerical calculation for the exact field and the far field.

2. First-order spatial coherence

Let us suppose that the emission of synchrotron radiation from each electron in the storage ring is chaotic. Then the correlation of two fields is written as

$$\begin{aligned}\langle E_i^*(x_1, z)\, E_j(x_2, z)\rangle = {}& \textstyle\int \mathrm{d}x_e \int \mathrm{d}\varphi_e\, \rho(x_e, \varphi_e) \\ & \times E_i^*(x_1, z, x_e, \varphi_e)\, E_j(x_2, z, x_e, \varphi_e),\end{aligned} \tag{1}$$

where $E_i(x, z, x_e, \varphi_e)$ is the electric field at (x, z) which has i polarization and is emitted by an electron whose phase space coordinate is (x_e, φ_e), where x_e and φ_e are the electron coordinate and the divergence at the emitting point, respectively.† We assume that the electric field travels towards the z direction and that the x direction is perpendicular to the z direction and the phase spaces for x and y directions are independent. For this reason we consider only the x direction for the spatial coherence here. We also assume that the electric field should be well monochromatic and we regard the coherent time to be infinity. $\rho(x_e, \varphi_e)$ is the electron distribution function in the storage ring and is given by

† In this paper we use the notation $\mathbf{x}$, $\vec{x}$ and x to represent the three-dimensional vector, the two-dimensional vector and just a coordinate, respectively.

$$\rho(x_e, \varphi_e) = (N_e/2\pi\varepsilon_e)\exp[-(\gamma x^2 + 2\alpha x\varphi + \beta\varphi^2)/2\varepsilon_e]. \quad (2)$$

N_e is proportional to the total number of electrons and ε_e is the electron beam emittance. α, β and γ are Twiss parameters at the emitting point which satisfy $\beta\gamma - \alpha^2 = 1$. ε_e is the electron beam emittance in the storage ring. The intensities at x_1, x_2, the correlation between the fields at x_1 and x_2, and the first-order coherence of them are given by

$$I(x_1, z) = \sum_i \langle E_i^*(x_1, z)\, E_i(x_1, z)\rangle, \quad (3)$$

$$I(x_2, z) = \sum_i \langle E_i^*(x_2, z)\, E_i(x_2, z)\rangle, \quad (4)$$

$$M(x_1, x_2, z) = \sum_i \langle E_i^*(x_1, z)\, E_i(x_2, z)\rangle, \quad (5)$$

$$\gamma(x_1, x_2, z) = M(x_1, x_2, z)/[I(x_1, z)^{1/2} I(x_2, z)^{1/2}], \quad (6)$$

respectively (Born & Wolf, 1980). The visibility is defined as

$$V = \frac{2[I(x_1, z)I(x_2, z)]^{1/2}}{I(x_1, z) + I(x_2, z)}\,|\gamma(x_1, x_2, z)|. \quad (7)$$

This means that the visibility is proportional to the absolute value of the first-order coherence and is equivalent to it if the intensities at two points are equal. Hereafter, the first-order coherence and the visibility have the same meaning. In the realistic cases, because of the finite width of the double slit, the measured visibility by the Young's interferometer is

$$\overline{V} = 2|\overline{M(x_1, x_2)}|/[\overline{I(x_1, z)} + \overline{I(x_2, z)}], \quad (8)$$

where

$$\overline{I(x_1)} = \int_{-d/2}^{d/2} \mathrm{d}x \int_{-d/2}^{d/2} \mathrm{d}x'\, M(x_1 + x, x_1 + x'), \quad (9)$$

$$\overline{I(x_2)} = \int_{-d/2}^{d/2} \mathrm{d}x \int_{-d/2}^{d/2} \mathrm{d}x'\, M(x_2 + x, x_2 + x'), \quad (10)$$

$$\overline{M(x_1, x_2, z)} = \int_{-d/2}^{d/2} \mathrm{d}x \int_{-d/2}^{d/2} \mathrm{d}x'\, M(x_1 + x, x_2 + x'), \quad (11)$$

and d is the width of the slit. In general, V and $\overline{V}$ are not equal. However, we consider the ideal cases where d is infinitesimally narrow and V and $\overline{V}$ can be regarded as the same.

The brightness is another important quantity which is closely related to the first-order coherence (Kim, 1986). It has an analogy with the Wigner function and is written as

$$B_{ij}(x, \varphi, z) = C_0 \int \mathrm{d}y\, \langle E_i^*(x + y/2, z)\, E_j(x - y/2, z)\rangle \times \exp(ik\varphi y) \quad (12)$$

$$= \int \mathrm{d}x_e \int \mathrm{d}\varphi_e\, \rho(x_e, \varphi_e)\, B_{ij}^{(0)}(x, \varphi, z, x_e, \varphi_e), \quad (13)$$

where k is the wave number and C_0 is a constant.

$$B_{ij}^{(0)}(x, \varphi, z, x_e, \varphi_e) = C_0 \int \mathrm{d}y\, E_i^*(x + y/2, z, x_e, \varphi_e) \times E_j(x - y/2, z, x_e, \varphi_e)\exp(ik\varphi y) \quad (14)$$

is the brightness in the case where a single electron exists only at (x_e, φ_e) in the phase space.

3. Gaussian beam

Gaussian optics are very useful because of their similarities with the geometrical optics in the limiting case and because they are easy to treat analytically. We define the transfer matrix from the light source ($z = z_0$) to the observation point ($z = z_1$) in the linear approximation as

$$T(z_0, z_1) = \begin{pmatrix} a & b \\ c & d \end{pmatrix}, \quad (ad - bc = 1). \quad (15)$$

Then the brightness transforms as

$$B(x, \varphi, z_1) = B(dx - b\varphi, -cx + a\varphi, z_0), \quad (16)$$

in the case of the Gaussian optics (Kim, 1986). Here we neglected the indices of the polarization supposing that the Gaussian beam has only one component of the polarization. At $z = z_0$ we put

$$B^{(0)}(x, \varphi, z_0, x_e, \varphi_e) = (B_0/2\pi\sigma_p\sigma_p')\exp\{[-(x - x_e)^2/2\sigma_p^2] - [(\varphi - \varphi_e)^2/2\sigma_p'^2]\}, \quad (17)$$

for (14). In (17), B_0 is a constant and σ_p and σ_p' are the beam size and the beam divergence of a single photon, respectively, which satisfy

$$\sigma_p\sigma_p' = \lambda/4\pi. \quad (18)$$

From (14), (16) and (17), the electric field is determined by

$$E(x, z_1, x_e, \varphi_e) = E_0\exp\{-[Ax^2 + 2Bx + C^{(r)}]/4\}, \quad (19)$$

with

$$A^{(r)} = 1/\bar{\sigma}_p^{\,2}, \quad (20)$$

$$A^{(i)} = -2k(bd\sigma_p'^2 + ac\sigma_p^2)/\bar{\sigma}_p^{\,2}, \quad (21)$$

$$B^{(r)} = -(ax_e + b\varphi_e)/\bar{\sigma}_p^{\,2}, \quad (22)$$

$$B^{(i)} = 2k(b\sigma_p'^2 x_e - a\sigma_p^2\varphi_e)/\bar{\sigma}_p^{\,2}, \quad (23)$$

$$C^{(r)} = (ax_e + b\varphi_e)^2/\bar{\sigma}_p^{\,2}, \quad (24)$$

$$|E_0|^2 = B_0/[2\pi(8\pi)^{1/2}\bar{\sigma}_p\sigma_p\sigma_p'], \quad (25)$$

$$\bar{\sigma}_p = (a^2\sigma_p^2 + b^2\sigma_p'^2)^{1/2}, \quad (26)$$

where indices (r) and (i) denote the real and the imaginary parts, respectively. The overall phase in (19), which is not important for calculating (1) or (13), is omitted. In other words, the expression for the brightness with (16) and (17) is equivalent to approximating the electric field by (19) which is the Gaussian beam.

From the Fourier inverse transformation of (12), (13) and (17) we have

$$\begin{aligned}\langle E^*(x_1,z_1)E(x_2,z_1)\rangle &= (k/2\pi C_0)\textstyle\int \mathrm{d}\varphi \\ &\quad\times B[(x_1+x_2)/2,\varphi,z_1] \\ &\quad\times \exp[-ik\varphi(x_1-x_2)] \\ &= N_e|E_0|^2(\bar{\sigma_p}/\bar{\Sigma})\exp\{-[g_1(x_1^2+x_2^2) \\ &\quad+2g_2x_1x_2+ig_3(x_1^2-x_2^2)]\},\end{aligned} \tag{27}$$

where $\bar{\Sigma}$ is the beam size at $z=z_1$ given by

$$\bar{\Sigma}=[a^2(\sigma_p^2+\beta\varepsilon_e)+b^2(\sigma_p'^2+\gamma\varepsilon_e)-2ab\alpha\varepsilon_e]^{1/2}, \tag{28}$$

and

$$g_1=(\varepsilon^2+\varepsilon_p^2)/8\bar{\Sigma}^2\varepsilon_p^2, \tag{29}$$

$$g_2=(\varepsilon^2-\varepsilon_p^2)/8\bar{\Sigma}^2\varepsilon_p^2, \tag{30}$$

$$g_3=(k/2\bar{\Sigma}^2)[bd(\sigma_p'^2+\gamma\varepsilon_e)+ac(\sigma_p^2+\beta\varepsilon_e)-\alpha(ad+bc)\varepsilon_e]. \tag{31}$$

From (7) and (27) we have a useful expression of the visibility,

$$V=[1/\cosh(Dx_c/2\bar{\Sigma}^2)]\exp(-D^2/8\sigma_c^2), \tag{32}$$

where

$$x_c=(x_1+x_2)/2, \tag{33}$$

$$D=|x_1-x_2|, \tag{34}$$

and σ_c is the coherent size given by

$$\sigma_c=\varepsilon_p\bar{\Sigma}/(\varepsilon^2-\varepsilon_p^2)^{1/2}. \tag{35}$$

Here we used the definitions of a single photon beam emittance, ε_p, and the total photon beam emittance, ε,

$$\varepsilon_p=\sigma_p\sigma_p'=\lambda/4\pi, \tag{36}$$

and

$$\varepsilon=(\varepsilon_e^2+\gamma\varepsilon_e\sigma_p^2+\beta\varepsilon_e\sigma_p'^2+\varepsilon_p^2)^{1/2}. \tag{37}$$

Obviously the expression of the visibility in (32) is also obtained directly from (1) and (19). It should be noted that (35) contains the Twiss parameters and the transfer matrix only through the beam size $\bar{\Sigma}$ and the total photon emittance ε. Therefore, if the beam size $\bar{\Sigma}$ and the coherent size σ_c are measured, the total photon beam emittance ε can be known without any knowledge of the Twiss parameters, β,γ or the transfer matrix. Moreover, if one can measure ε for three different photon energies, one can know in principle the Twiss parameters and the electron beam emittance ε_e.

In this section we have used the fact that a Gaussian beam can be treated in the linear approximation. We supposed that the synchrotron radiation beam also can be treated in the linear approximation, which seems to be reasonable as the synchrotron radiation beam has a sharp directional property. We will derive a general condition for the electric field to be treated in the linear approximation. To investigate the brightness which transforms linearly, we consider a brightness function of a single electron, $B(\vec{x},\vec{\varphi},z)$, where $\vec{x}$ and $\vec{\varphi}$ are two-dimensional vectors which are the position in the transverse plane and the divergence. If we write the transfer matrix as

$$T(z,z+\epsilon)=\begin{pmatrix}1 & \epsilon\\ 0 & 1\end{pmatrix}, \tag{38}$$

then T represents the transformation from z to $z+\epsilon$ in free space. From (16), the brightness transforms as

$$B(\vec{x},\vec{\varphi},z+\epsilon)=B(\vec{x}-\epsilon\vec{\varphi},\vec{\varphi},z). \tag{39}$$

In the limit $\epsilon\to 0$, (39) can be rewritten by a differential equation

$$(\partial/\partial z+\vec{\varphi}.\partial/\partial\vec{x})\,B(\vec{x},\vec{\varphi},z)=0. \tag{40}$$

If we substitute the definition of the brightness of a single electron,

$$\begin{aligned}B(\vec{x},\vec{\varphi},z)&=C_0\textstyle\int \mathrm{d}\vec{y}\,E^*\big(\vec{x}+\vec{y}/2,z\big)E\big(\vec{x}-\vec{y}/2,z\big)\\ &\quad\times\exp(ik\vec{\varphi}.\vec{y}),\end{aligned} \tag{41}$$

into (40), we obtain a differential equation,

$$\begin{aligned}&E^*(\vec{x_2},z)\big(\Delta_{\vec{x_1}}+2ik\,\partial/\partial z\big)\,E(\vec{x_1},z)\\ &\quad+E(\vec{x_1},z)\big(\Delta_{\vec{x_2}}-2ik\,\partial/\partial z\big)\,E^*(\vec{x_2},z)=0,\end{aligned} \tag{42}$$

where

$$\Delta_{\vec{x}}=\partial/\partial\vec{x}.\partial/\partial\vec{x}. \tag{43}$$

As $\vec{x_1}$ and $\vec{x_2}$ are independent variables, we have

$$(\Delta_{\vec{x}}+2ik\,\partial/\partial z+i\zeta)\,E(\vec{x},z)=0, \tag{44}$$

where ζ is a real constant. For $\zeta=0$ in (44), we obtain the paraxial equation

$$(\Delta_{\vec{x}}+2ik\,\partial/\partial z)\,E(\vec{x},z)=0, \tag{45}$$

which is also obtained from the Maxwell equation if the dependence of the field on z can be approximated by the plane wave (Mandel & Wolf, 1995). It is noted that the Gaussian beam is a solution of (45). As synchrotron radiation can be regarded as a plane wave along the optical axis owing to its directional property, it is reasonable to treat synchrotron radiation in the linear approximation.

4. Basic theory of synchrotron radiation

To calculate the electric field we use the following formula (Jackson, 1962),

$$\begin{aligned}\mathbf{E}(\mathbf{x})&=(2\pi)^{-1/2}(e/4\pi\varepsilon_0)\textstyle\int \mathrm{d}t\,\exp(i\omega t)\\ &\quad\times\big[(\mathbf{n}/\kappa R^2)+(1/c\kappa)(d/dt')(\mathbf{n}-\beta)/\kappa R)\big]_{t=t'+R/c},\end{aligned} \tag{46}$$

where e, c and ε_0 are the electron charge, the light velocity and the dielectric constant, respectively. $\mathbf{x}=(\vec{x},z)$ is the observation point and $\vec{x}$ is a two-dimensional vector. $\mathbf{n}$ and R are the unit vector and the distance between the observer and an electron, respectively. β is the electron velocity normalized by c, and κ is defined by $(1-\beta.\mathbf{n})$. ω is the angular frequency of the photon which we observe. In general, the electric field at $z=z_1$, which was induced by an electron whose phase space coordinate was $(\vec{x}_e, \vec{\varphi}_e)$, where $\vec{x}_e$ and $\vec{\varphi}_e$ are two-dimensional vectors, and has travelled through the free space from $z=z_0=0$ to $z=z_1=L$, is given by

$$\mathbf{E}(\vec{x}, L, x_e, \varphi_e) = \mathbf{E}\big[\vec{x} - (\vec{x}_e + L\vec{\varphi}_e), L\big]\exp(ik\vec{\varphi}_e.\vec{x}). \quad (47)$$

We can numerically calculate the first-order coherence from (7), (46) and (47) by specifying the electron trajectory in the storage ring. Before the calculation, we will investigate a limiting case of the field pattern in (46). The far-field pattern of synchrotron radiation from the undulator is approximately written as (Alferov *et al.*, 1973, 1974; Kincaid, 1977)

$$E(\vec{x}, L) \simeq \sin[N\pi\psi(\vec{x})]/N\sin[\pi\psi(\vec{x})] \times \exp\Big[i(k\vec{x}^2/2L) + i(N-1)\pi\psi(\vec{x})\Big]f_u(\vec{x}), \quad (48)$$

where

$$\psi(\vec{x}) = (\omega/\omega_1)\Big[1 + \Big(\gamma_e^2\vec{x}^2/\big\{L^2[1+(K_x^2+K_y^2)/2]\big\}\Big)\Big], \quad (49)$$

$$\omega_1 = \big\{2\gamma_e^2/\big[1+(K_x^2+K_y^2/2)\big]\big\}(2\pi c/\lambda_u), \quad (50)$$

and K_x, K_y, N, λ_u are the K value for the x direction, the K value for the y direction, the number of the periods and the length of a period of the undulator, respectively. ω and k are the angular frequency and the wave number of the photon to be observed, respectively, which satisfy $\omega = ck$. γ_e is the electron energy normalized by the electron rest mass. ω_1 is the angular frequency of the first harmonic observed on the axis. $f_u(\vec{x})$ is a slowly varying function of $\vec{x}$ compared with the other terms. We have neglected the polarizations of the electric fields for the far-field case of the undulator. The phase terms in (48) are due to the spherical wave nature and the interference of each period. The first term changes much more rapidly than the second term. Therefore, in the far-field approximation the synchrotron radiation from the undulator is characterized by a spherical wave and the beam profile which has a form $[\sin(Nx)/\sin(x)]^2$ but not $\exp(-x^2)$.

The far-field pattern of the synchrotron radiation from a bending magnet is written as (Jackson, 1962; Schwinger, 1949)

$$E_\sigma(y, L) \simeq f_b(\omega/\omega_c)\big[1+W^2(y)\big]K_{2/3}[\eta(y)]\exp\big(iky^2/2L\big), \quad (51)$$

and

$$E_\pi(y, L) \simeq f_b(\omega/\omega_c)[1+W^2(y)]\big\{iW(y)/[1+W^2(y)]\big\} \times K_{1/3}[\eta(y)]\exp\big(iky^2/2L\big), \quad (52)$$

where

$$W(y) = \gamma_e y/L, \quad (53)$$

$$\eta(y) = (\omega/2\omega_c)\big[1+W^2(y)\big]^{3/2}, \quad (54)$$

and

$$\omega_c = 3\gamma_e^3 c/2\rho. \quad (55)$$

ω_c is the critical angular frequency and ρ is the bending radius. $K_{2/3}(x)$ and $K_{1/3}(x)$ are modified Bessel functions whose orders are 2/3 and 1/3, respectively. f_b is an unimportant constant. ω and k are the angular frequency and the wave number of the photon, respectively. As the horizontal distribution of the synchrotron radiation from the bending magnet is regarded to be uniform, we have considered only the vertical direction y. The beam profile of the σ polarization component is very similar to the Gaussian shape, while the π component has the minimum value at the centre.

5. Coherence of synchrotron radiation from the undulator

We have derived a useful formula of the visibility in the Gaussian approximation in §3. Strictly speaking, the electric field of the synchrotron radiation cannot be regarded as a Gaussian beam. Therefore we need to compare the visibilities of the actual synchrotron radiation and the Gaussian beam to approximate the actual synchrotron radiation.

First we consider the helical undulator case. In order to use the Gaussian approximation we must know the electron distribution function, ε_p, ε and $\bar{\Sigma}$. We suppose that the electron distribution function is already known. ε_p, which is the intrinsic photon beam emittance, can be calculated from (36) if we choose the photon energy. As the beam size produced by a single electron at $z=L$ is almost $L\sigma'_p$ when L is so large that the far-field approximation can be applied, σ'_p can be obtained by fitting the whole beam profile with the Gaussian shape $\exp\big(-x^2/2L^2\sigma_p'^2\big)$. Here we use the Marquardt–Levenberg algorithm for the fitting. σ_p can be calculated from (36). Then, ε is calculated from (37). $\bar{\Sigma}$ can be calculated by fitting the beam size produced by all electrons with the Gaussian shape $\exp\big(-x^2/2\bar{\Sigma}^2\big)$, where the fields are calculated exactly using (46).

We calculated the visibility from (32) and compared this result with the exact calculation of the visibility by (13) and (46). We also calculated the visibility for the simple far-field approximation using (48), *i.e.* using a non-Gaussian beam with the form $[\sin(Nx)/\sin(x)]^2$. This calculation is easier than the exact calculation because the analytic form is known for the far field. The far-field calculation and the exact calculation should give the same results at the far point. We defined $\sigma_c(E)$, $\sigma_c(F)$ and $\sigma_c(G)$, which are the coherent sizes given by the exact field, the far field and the Gaussian field, respectively. These values are calculated by fitting the visibility curves with the Gaussian shape in (32). We will summarize three methods mentioned above.

5.1. *Exact calculation*

This is a procedure where the fields are *exactly* calculated and the results are fitted to (32) *approximately* as follows.

(i) Decide the Twiss parameters, the electron emittance and the photon energy.

(ii) Calculate the fields using (46) for many electrons in the phase space and take the ensemble average for the correlation of the two fields in (1).

(iii) Calculate the beam size $\bar{\Sigma}$ by fitting the beam profile with the Gaussian. This is not necessary for calculating the coherent size in the exact calculation but in the Gaussian approximation.

(iv) Fit the visibility curve with the Gaussian shape in (32) and calculate the coherent size $\sigma_c(E)$.

5.2. *Far-field approximation*

This is a procedure where the fields are calculated using the *far-field approximation* and the results are fitted to (32) *exactly* as follows.

(i) Decide the Twiss parameters, the electron emittance and the photon energy.

(ii) Calculate the fields using (47) and (48) for many electrons in the phase space and take the ensemble average for the correlation of the two fields in (1).

(iii) Fit the visibility curve with the Gaussian shape in (32) and calculate the coherent size $\sigma_c(F)$.

5.3. *Gaussian approximation*

This is a procedure where the fields are calculated using the *Gaussian approximation* and the results are fitted to (32) *exactly* as follows.

(i) Decide the Twiss parameters, the electron emittance and the photon energy.

(ii) Calculate σ_p' by fitting the far-field pattern with the Gaussian shape and calculate σ_p using (36).

(iii) Calculate the coherent size $\sigma_c(G)$ using (35).

The parameters are $N = 12$, $\gamma_e = 4892$, $K_x = K_y = 1.28$ and $\lambda_u = 160$ mm. The photon energy of the first harmonic is 140 eV. Although the beam profile of the undulator depends on the photon energy, we simply restrict to the first-harmonic energy. The photon divergence and the size are calculated to be $\sigma_p' = 0.044$ mrad and $\sigma_p = 0.016$ mm, respectively. We chose two distances L from the centre of the undulator to the observation point as 2.04 m and 29.04 m. For the electron distribution function we set

$$\rho_e(x, \varphi, z) = (N_e/2\pi\sigma_e\sigma_e')\exp\left[-\left(x^2/\sigma_e^2 + \varphi^2/\sigma_e'^2\right)/2\right] \quad (56)$$

in (2), where σ_e and σ_e' are the beam size and the beam divergence at the entrance of the undulator. The electron beam emittance and the Twiss parameters are given by

$$\varepsilon_e = \sigma_e\sigma_e', \quad (57)$$

$$\sigma_e = (\beta\varepsilon_e)^{1/2}, \quad (58)$$

$$\sigma_e' = (\gamma\varepsilon_e)^{1/2}. \quad (59)$$

We simply put $x_c = 0$ and plotted the visibility as a function of $(D/\bar{\Sigma})$ which is the separation of two points. This plot is useful because the visibility depends on the transfer matrix only through $(D/\bar{\Sigma})$ for the Gaussian approximation as shown in (32) and (35).

To see how the visibility depends on the electron beam parameters, we separately set the electron beam size and the divergence at non-zero values, which are much larger

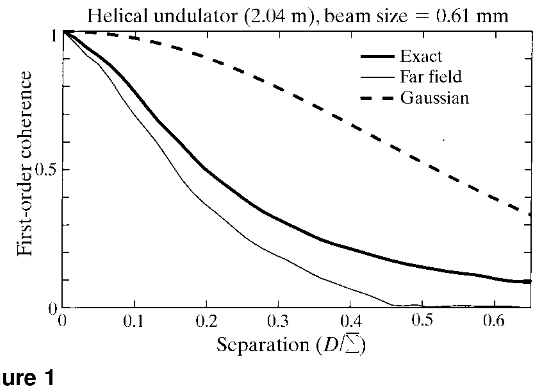

Figure 1
Coherence of synchrotron radiation from the helical undulator when $\sigma_e = 0$ mm, $\sigma_e' = 0.2$ mrad, $L = 2.04$ m with all polarizations observed. [$\sigma_c(E) = 0.060$ mm, $\sigma_c(F) = 0.044$ mm, $\sigma_c(G) = 0.13$ mm.]

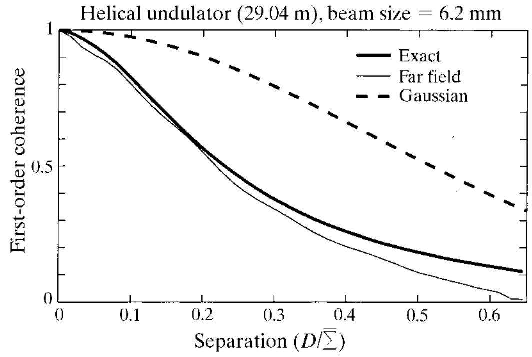

Figure 2
Coherence of synchrotron radiation from the helical undulator when $\sigma_e = 0$ mm, $\sigma_e' = 0.2$ mrad, $L = 29.04$ m with all polarizations observed. [$\sigma_c(E) = 0.70$ mm, $\sigma_c(F) = 0.63$ mm, $\sigma_c(G) = 1.4$ mm.]

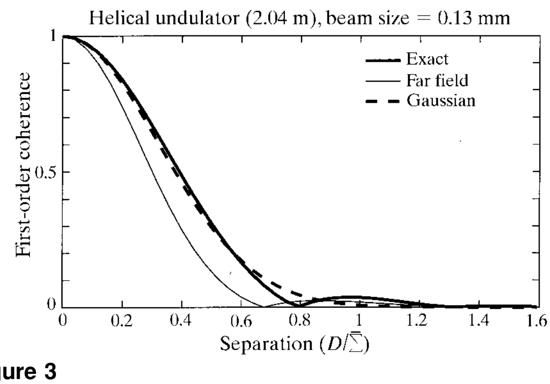

Figure 3
Coherence of synchrotron radiation from the helical undulator when $\sigma_e = 0.1$ mm, $\sigma_e' = 0$ mrad, $L = 2.04$ m with all polarizations observed. [$\sigma_c(E) = 0.020$ mm, $\sigma_c(F) = 0.016$ mm, $\sigma_c(G) = 0.020$ mm.]

than the beam size and the beam divergence of a single photon. Finally we set both of them at non-zero values.

First we calculated for $\sigma_e = 0$ mm, $\sigma'_e = 0.2$ mrad (Figs. 1 and 2). It can be seen that the first-order coherence of the Gaussian approximation is higher than that of the exact calculation and that the behaviours of the exact calculation and the far-field approximation are very similar. This implies that the first-order coherence is very sensitive to the beam shape. The small discrepancy for the exact calculation and the far-field calculation at L = 29.04 m has occurred because the distance L = 29.04 m is not very large. Another reason is that an electron with a different angular divergence experiences a different magnetic field in the exact calculation. This effect is not taken into account in the far-field approximation and the Gaussian approximation.

Next we calculated for $\sigma_e = 0.1$ mm, $\sigma'_e = 0$ mrad (Figs. 3 and 4). The Gaussian approximation has good agreement with the exact calculation and the far-field approximation. Therefore, if the electron beam divergence can be almost neglected, which means $\sigma'_e \ll \sigma'_p$, one can regard the synchrotron radiation from the undulator as a Gaussian beam in terms of the coherence.

The asymmetry of the effects on the coherence by the electron beam divergence and the beam size can be understood by using (32). We consider the special two cases where the divergence of the electron beam can be neglected compared with σ'_p and where the beam size of the electron beam can be neglected compared with σ_p at the emitting point. If we put the transfer matrix

$$T(z_0, z_0 + L) = \begin{pmatrix} 1 & L \\ 0 & 1 \end{pmatrix}, \tag{60}$$

and $\sigma_e \neq 0$, $\sigma'_e = 0$, we have

$$V = \exp\{-\sigma_e^2 D^2/[8\sigma_p^2(\sigma_p^2 + \sigma_e^2 + L^2\sigma_p'^2)]\}, \tag{61}$$

for the visibility in (32). On the other hand, if we put $\sigma_e = 0$, $\sigma'_e \neq 0$, then the visibility can be written as

$$V = \exp\left(-\sigma_e'^2 D^2/\{8\sigma_p'^2[\sigma_p^2 + L^2(\sigma_p'^2 + \sigma_e'^2)]\}\right). \tag{62}$$

For $L^2 \gg (\sigma_p^2 + \sigma_e^2)/(\sigma_p'^2 + \sigma_e'^2)$, (61) and (62) are reduced to

$$V = \exp\left(-2\pi^2\sigma_e^2 D^2/\lambda^2 L^2\right), \tag{63}$$

and

$$V = \exp\{-\sigma_e'^2 D^2/[8\sigma_p'^2(\sigma_p'^2 + \sigma_e'^2)L^2],\tag{64}$$

respectively. Here we used (18) in (63). The visibility in (63) does not depend on the beam profile of a single photon but only on the wavelength. However, the visibility in (64) explicitly depends on σ'_p, which means the visibility is sensitive to the beam shape of a single photon in this case. Figs. 5 and 6 are the cases for $\sigma_e = 0.1$ mm, $\sigma'_e = 0.2$ mrad, both of which are much larger than those of a single photon. We compared the Gaussian approximation and the far-field approximation which should give almost the same result as the exact calculation. The disagreement of the calculated coherence is larger than that of the case for $\sigma_e =$ 0.1 mm, $\sigma'_e = 0$ mrad, but smaller than that of the case for $\sigma_e =$ 0 mm, $\sigma'_e =$ 0.2 mrad, as expected from the above discussion.

Even if we take only one component of the polarization, the results are almost the same with the cases taking all polarizations for the helical undulator. This is because the polarization of the helical undulator is almost uniform and the coherence is high within the transverse plane where

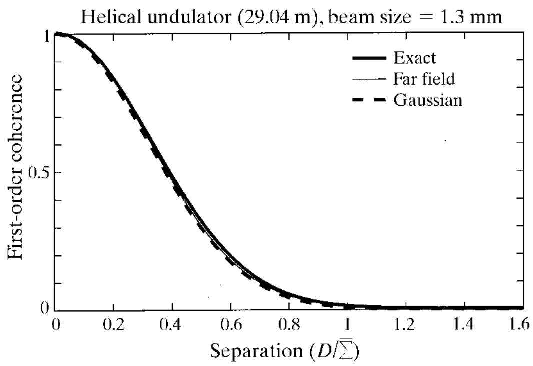

Figure 4
Coherence of synchrotron radiation from the helical undulator when $\sigma_e = 0.1$ mm, $\sigma'_e = 0$ mrad, L = 29.04 m with all polarizations observed. [$\sigma_c(E) = 0.21$ mm, $\sigma_c(F) = 0.20$ mm, $\sigma_c(G) = 0.20$ mm.]

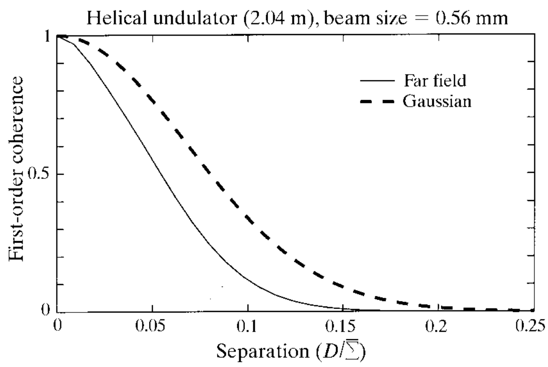

Figure 5
Coherence of synchrotron radiation from the helical undulator when $\sigma_e = 0.1$ mm, $\sigma'_e = 0.2$ mrad, $L = 2.04$ m with all polarizations observed. [$\sigma_c(F) = 0.013$ mm, $\sigma_c(G) = 0.019$ mm.]

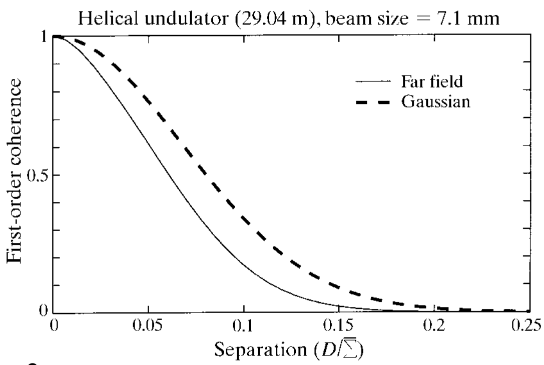

Figure 6
Coherence of synchrotron radiation from the helical undulator when $\sigma_e =$ 0.1 mm, $\sigma'_e =$ 0.2 mrad, $L =$ 29.04 m with all polarizations observed. [$\sigma_c(F) = 0.18$ mm, $\sigma_c(G) = 0.24$ mm].

most of the total intensity is concentrated because of the small K value.

6. Coherence of synchrotron radiation from the bending magnet

For synchrotron radiation from the bending magnet, we compared the first-order coherence of the far-field approximation equations (51) and (52) with that of the Gaussian approximation (Fig. 7, Fig. 8 and Fig. 9). We calculated σ_p, σ'_p and $\bar{\Sigma}$ as we did in the previous section. We chose L = 29.04 m for the following three cases: all polarizations, σ polarization and π polarization, where we took the electron parameters as $\sigma_e = 0$ mm and $\sigma'_e = 0.2$ mrad. We set the parameters as $\gamma_e = 4892$, $\rho = 8.66$ m and a critical energy of 4 keV. The photon energy to be observed is 140 eV. The first-order coherence depends strongly on the polarization because the polarization changes from one to another on the transverse plane in this case. The case for σ polarization is almost similar to the Gaussian beam as its beam shape looks Gaussian near the optical axis.

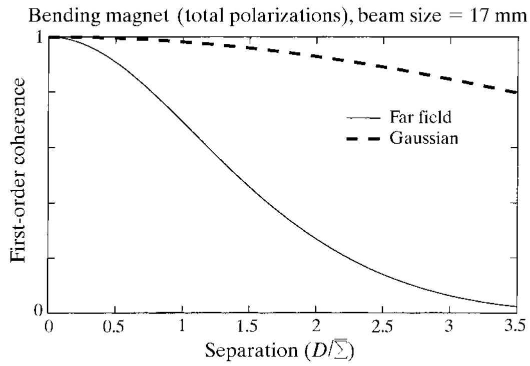

Figure 7
Coherence of synchrotron radiation from the bending magnet when $\sigma_e = 0$ mm, $\sigma'_e = 0.2$ mrad, $L = 29.04$ m with all polarizations observed. [$\sigma_c(F) = 10$ mm, $\sigma_c(G) = 44$ mm.]

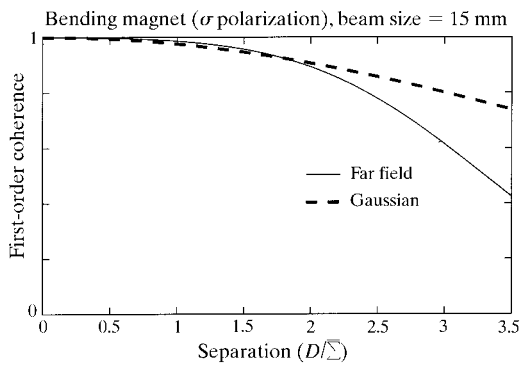

Figure 8
Coherence of synchrotron radiation from the bending magnet when $\sigma_e = 0$ mm, $\sigma'_e = 0.2$ mrad, $L = 29.04$ m with σ polarization observed. [$\sigma_c(F) = 21$ mm, $\sigma_c(G) = 33$ mm.]

Because the component for π polarization has two maxima and the phases of them are opposite, the behaviour of the first-order coherence for π polarization is very strange and decreases to zero for the finite separation length. One can understand this situation by regarding the far field as a simple superposition of two Gaussian beams, which is

$$E(x, z = L, 0, 0) = E_0\{\exp[-(x - x_0)^2/4\sigma^2] - \exp[-(x + x_0)^2/4\sigma^2]\} \times \exp(ikx^2/2L), \qquad (65)$$

where x_0 and σ are the absolute value of the position of the maxima and the beam size of each Gaussian beam, respectively. One can calculate the first-order coherence from (1), (7) and (65), and the result is

$$V = \exp[-(k^2\sigma_e^2/2\kappa_a^2 + 1/8\kappa_b^2)D^2]|v(D)|, \qquad (66)$$

where

$$v(D) = [\exp(x_0^2/2\kappa_b^2)\cos(k\sigma_e^2 Dx_0/\bar{\Sigma}^2 L) - \cosh(Dx_0/2\sigma^2)] \times [\exp(x_0^2/2\kappa_b^2)\cosh(Dx_0/2\bar{\Sigma}^2) - 1]^{-1}. \qquad (67)$$

Here, we put

$$\bar{\Sigma} = (\sigma_e^2 + \sigma^2 + L^2\sigma_e'^2)^{1/2}, \qquad (68)$$

$$1/\kappa_a^2 = (\sigma^2 + L^2\sigma_e'^2)/L^2\bar{\Sigma}^2, \qquad (69)$$

$$1/\kappa_b^2 = (\sigma_e^2 + L^2\sigma_e'^2)/\sigma^2\bar{\Sigma}^2. \qquad (70)$$

If $x_0 \neq 0$, one can verify

$$v(0) = 1, \qquad (71)$$

$$\lim_{D\to\infty} v(D) = -1, \qquad (72)$$

and $v(D)$ is a smooth function for $D \geq 0$. As a result, $v(D)$ must take zero value for finite D, where V also has zero value. The essential point is that the two maxima of the field are in opposite phases, which makes the correlation average to zero at some finite D.

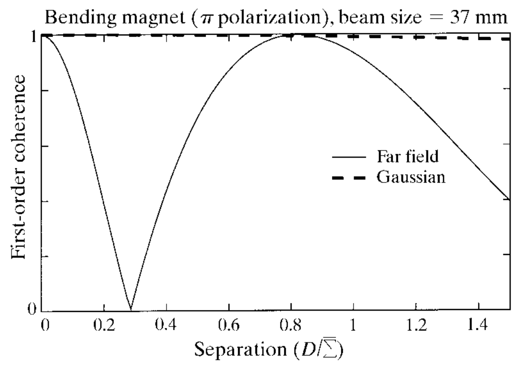

Figure 9
Coherence of synchrotron radiation from the bending magnet when $\sigma_e = 0$ mm, $\sigma'_e = 0.2$ mrad, $L = 29.04$ m with π polarization observed. [$\sigma_c(F) = 24$ mm, $\sigma_c(G) = 13$ mm.]

For any polarizations, the coherence for the exact field is smaller than that for the Gaussian beam.

7. Conclusions

We have obtained an analytic form of the first-order coherence for the Gaussian beam and compared this with that of the actual synchrotron radiation beam. We have shown that the total photon beam emittance can be obtained by measuring the beam size and the coherent size in the Gaussian approximation [equation (35)]. It seems that the Gaussian approximation has some limitations when calculating the coherence. The quantitative argument is not so clear for the Gaussian approximation, while the far-field approximations gives almost correct values for the coherence even for the near-field cases. This means that it might be possible to find a simple representation of the coherence by using the far-field approximation, which is not so complicated. We have discussed only the free-field cases but the generalization to other optical devices may not be so difficult. The estimation of the electron beam emittance from the calculation in this paper and the experiment will be described elsewhere.

References

Alferov, D. F., Bashmakov, Y. A. & Bessonov, E. G. (1973). *Zh. Tekh. Fiz.* **43**, 2126–2129.

Alferov, D. F., Bashmakov, Y. A. & Bessonov, E. G. (1974). *Sov. Phys. Tech. Phys.* **18**, 1336–1339.

Born, M. & Wolf, E. (1980). *Principle of Optics*, ch. 10. New York: Pergamon Press.

Coisson, R. (1995). *Appl. Opt.* **34**, 904–908.

Hatano, T., Okamoto, W., Miyahara, T. & Takayama, Y. (1998). In preparation.

Jackson, J. D. (1962). *Classical Electrodynamics*, ch. 14. New York: John Wiley.

Kim, K.-J. (1986). *Nucl. Instrum. Methods*, A**246**, 71–76.

Kincaid, B. M. (1977). *J. Appl. Phys.* **48**, 2684–2691.

Mandel, L. & Wolf, E. (1995). *Optical Coherence and Quantum Optics*, ch. 4. Cambridge University Press.

Schwinger, J. (1949). *Phys. Rev.* **75**, 1912–1925.